Available online at www.sciencedirect.com
SCIENCE DIRECT
Physics Letters B 635 (2006) 17–22
PHYSICS LETTERS B
www.elsevier.com/locate/physletb

Investigation of the $^{9}\mathrm{Li} + {}^{2}\mathrm{H} \rightarrow {}^{8}\mathrm{Li} + \mathrm{t}$ reaction at REX-ISOLDE

H.B. Jeppesen [a,b,*], A.M. Moro [c], T. Nilsson [d], F. Ames [e], P. van den Bergh [f], U.C. Bergmann [b], G. Bollen [g], M.J.G. Borge [h], J. Cederkäll [b], P. Van Duppen [f], S. Emhofer [e], O. Forstner [b], L.M. Fraile [b], H.O.U. Fynbo [a], J. Gómez-Camacho [c], D. Habs [e], R. von Hahn [i], G. Huber [j], M. Huyse [f], H.T. Johansson [k], B. Jonson [k], O. Kester [e], H. Lenske [l], L. Liljeby [m], M. Meister [k], G. Nyman [k], M. Oinonen [b], M. Pantea [d], H. Podlech [n], U. Ratzinger [n], K. Reisinger [e], K.G. Rensfelt [m], R. Repnow [i], K. Riisager [a,b], A. Richter [d], K. Rudolph [e], H. Scheit [i], A. Schempp [n], P. Schmidt [j], G. Schrieder [d], D. Schwalm [i], T. Sieber [e], H. Simon [d], O. Tengblad [h], E. Tengborn [k], M. Turrión [h], L. Weissmann [g], F. Wenander [b], B. Wolf [j]

[a] *Institut for Fysik og Astronomi, Aarhus Universitet, DK-8000 Aarhus C, Denmark*
[b] *ISOLDE, PH Department, CERN, CH-1211 Genéve 23, Switzerland*
[c] *Departamento de FAMN, Universidad de Sevilla, Apt 1065, 41080 Sevilla, Spain*
[d] *Institut für Kernphysik, Technische Universität Darmstadt, Schlossgartenstr. 9, D-64289 Darmstadt, Germany*
[e] *Ludwig Maximilians Universität München, Am Coulombwall 1, D-85748 Garching, Germany*
[f] *IKS, K.U. Leuven, Celestijnenlaan 200D, B-3001 Leuven, Belgium*
[g] *NSCL, Michigan State University, East Lansing, MI 48284, USA*
[h] *Instituto Estructura de la Materia, CSIC, E-28006 Madrid, Spain*
[i] *MPI für Kernphysik, Postfach 103980, D-69029 Heidelberg, Germany*
[j] *Johannes-Gutenberg-Universität, D-55099 Mainz, Germany*
[k] *Fundemental Fysik, Chalmers Tekniska Högskola, S-412 96 Göteborg, Sweden*
[l] *Institut für Theoretische Physik, Universität Giessen, D-35392, Germany*
[m] *Manne Siegbahn Laboratory, Frascativägen 24, S-10405 Stockholm, Sweden*
[n] *Institut für Angewandte Physik, Johann Wolfgang Goethe-Universität Frankfurt, Robert-Mayer-Str. 2-4, D-60325 Frankfurt, Germany*

Received 14 November 2005; received in revised form 27 January 2006; accepted 8 February 2006

Available online 23 February 2006

Editor: V. Metag

Abstract

The one-neutron transfer reaction $^{9}\mathrm{Li} + {}^{2}\mathrm{H} \rightarrow {}^{8}\mathrm{Li} + \mathrm{t}$ has been investigated in an inverse kinematics experiment by bombarding a deuterated polypropylene target with a 2.36 MeV/u ^{9}Li beam from the post-accelerator REX-ISOLDE at CERN. Excitation energies in ^{8}Li as well as angular distributions of the tritons were obtained and spectroscopic factors deduced.

PACS: 25.60.Je; 25.45.Hi; 27.20.+n

Keywords: NUCLEAR REACTIONS; RADIOACTIVE beam ^{9}Li (from Ta(p, x) reaction); REX-ISOLDE post-accelerator; C_3D_6 target; Measured outgoing tritons; Deduced excitation energy in ^{8}Li; $d\sigma/d\Omega$; DSSSD detector

1. Introduction

Transfer reactions with light and heavy ions have traditionally been a major source of spectroscopic information on nuclei at and near the line of stability [1,2]. With the recent devel-

* Corresponding author.
E-mail address: henrik.jeppesen@cern.ch (H.B. Jeppesen).

0370-2693
doi:10.1016/j.physletb.2006.02.034

opments of accelerated radioactive beams, of low energy at ISOL facilities, the study of exotic nuclei far from the valley of beta-stability, has now become possible via transfer reactions employing radioactive beams. As in the case of stable nuclei, transfer reactions can be used to extract spectroscopic information of exotic nuclei for both bound and unbound states [3]. Several new features for transfer reactions with radioactive beams have been predicted as, for example, a maximal transfer cross section at low incident energies and that the mechanism favours transfer reactions into excited states in the final nuclei [4]. Such features are directly related to the properties of the wave functions in weakly bound nuclei. The experimental development has been matched by significant progress in ab initio calculations of the structure of light nuclei [5] and the combination of experiment and theory allows new exacting tests to be performed. The nuclear structure interest on ^{8,9}Li is to understand the dynamics and spectroscopy of neutron-rich nuclei. Besides that the mass-8 isobar is of particular astrophysical interest because the understanding of these nuclei is the key to understand how the mass-8 bottleneck is overcome in primordial and stellar nucleosynthesis.

In this Letter we report on one example of an inverse kinematics experiment, namely a one-neutron transfer reaction experiment $^9\mathrm{Li} + {}^2\mathrm{H} \rightarrow {}^8\mathrm{Li} + \mathrm{t}$ performed at the REX-ISOLDE (Radioactive beam EXperiments at ISOLDE) post-accelerator at CERN.

2. Experimental setup

The ^{9}Li nuclei were produced at the CERN ISOLDE [6] facility by bombarding a Ta-foil target by a pulsed 1.4 GeV proton beam, with 3×10^{13} protons per pulse, and a maximum repetition rate of one pulse per 1.2 s. The ^{9}Li atoms were subsequently ionized in a surface ion-source and transferred to the REX-ISOLDE complex [7]. At REX-ISOLDE the 1^+ ions were first bunched in the REX-TRAP (20 ms cycles), then charge bred in REX-EBIS to the 2^+ charge state and finally accelerated to a energy of 2.36 MeV/u in the REX-LINAC.

The ^{9}Li beam entered the detector setup via a 4 mm diameter tungsten collimator and impinged on the 6.4 μm deuterated polypropylene reaction target ($(C_3D_6)_n$, 660 μg/cm^2). The charged particles were detected in a DSSSD-telescope (double sided silicon strip detector) placed off the beam axis covering laboratory angles from 18° to 80°, with an energy resolution of approximately 50 keV and an angular resolution about 3° [8] (for the triton channel the energy resolution in the excitation energy spectrum was about 0.7 MeV, see Fig. 1). The DSSSD-telescope consisted of a 16×16 strip (5×5 cm active area) DSSSD of 64 μm thickness backed by a 1000 μm Si pad detector. For a more detailed description of the beam conditions and detector setup see [9]. The overall normalization of the data has an uncertainty of 10% and the position of the DSSSD-telescope is uncertain to ±2°.

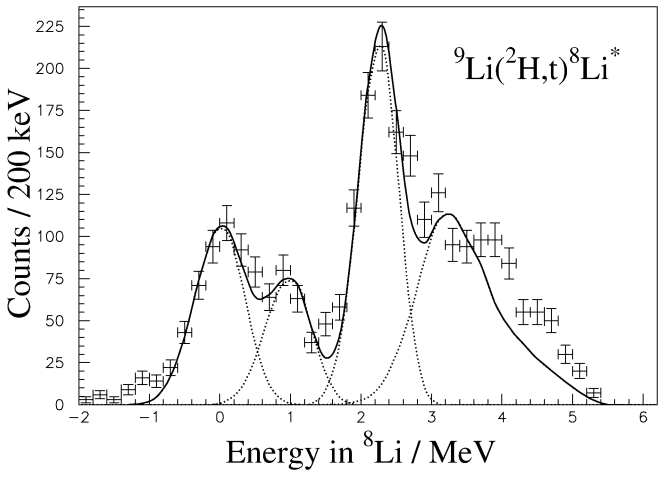

Fig. 1. Extracted excitation energy for identified tritons from the $^9\mathrm{Li} + {}^2\mathrm{H}$ reaction. The lines show simulations of the ground state and excited states at 0.9808, 2.2555 and 3.21 MeV in ^{8}Li (dotted) and their sum (solid).

3. Results and discussion

The charged particles observed from the $^9\mathrm{Li} + {}^2\mathrm{H}$ reaction were protons, deuterons, tritons, ^{4}He and ^{6}He, which could easily be separated. Here we shall concentrate on the triton channel where previously unobserved states should be present. The time distribution of the tritons published in [9] shows that this channel is free from stable background.

From the Q-value (2.2 MeV), energy and angular information it is straightforward to extract the excitation energy in ^{8}Li, assuming the reaction to be binary. The tritons could also originate from reactions between ^{9}Li and ^{12}C (10.8 MeV Q-value) this contribution would most likely be small and have a flat structureless distribution. For more information see Fig. 4E in [9] for a plot of the triton energy vs. laboratory scattering angle, on which kinematic lines are shown. The extracted excitation energy is shown in Fig. 1 together with simulations of the four lowest experimentally known states in ^{8}Li situated at 0 MeV, 0.9808 MeV, 2.2555 MeV and 3.21 MeV [10], as depicted in Fig. 2. Only the amplitudes for the four states have been varied to fit the spectrum shown in the figure. The simulations include energy and angular resolution and detector acceptance. The four single peaks (dotted lines in Fig. 1) are obtained by assuming that the three lowest states are narrow while the state at 3.21 MeV has been described in an R-matrix approach with an observed width of 1.5 MeV. Fig. 1 shows that the reproduction of the data is very good, at least up to energies of 3–3.5 MeV. The excess intensity at 4 MeV is briefly discussed later.

In the following we discuss the region above 3 MeV. From a single particle picture one expects that the lowest states in ^{8}Li are due to an unpaired proton and an unpaired neutron both in $1p_{3/2}$ orbits. This configuration can couple to 0^+, 1^+, 2^+ and 3^+, which should appear as the four lowest states in ^{8}Li. From the level scheme in Fig. 2 it is seen that no 0^+ state has been observed at low energy.

The next states which should appear in the ^{8}Li spectrum originate from the excitation of either the proton or neutron into the $1p_{1/2}$ orbit coupling to two pairs of 1^+ and 2^+ states. This

is the origin of the 1^+ state at 3.21 MeV, but the corresponding 2^+ state is still missing together with the second pair of 1^+ and 2^+ states.

Shell model and ab initio calculations of the position and spectroscopic factors of the low-lying levels in ^{8}Li have been performed. The shell model calculation has been done by Cohen and Kurath [11–13] and is given in Table 1 with label CK. Furthermore, ab initio calculations have been performed by Wiringa et al. with the Quantum Monte Carlo model [5] using the Argonne v_{18} + UrbanaIX interaction [14,15]. These results are listed in Table 1 labeled as QMC. From the table one can see that the qualitative picture discussed above concerning the grouping of the levels in ^{8}Li is confirmed in both calculations. The suggested position of the 0^+ state seems to be rather unclear and it will probably be very difficult to observe it via this reaction if it is situated around 2 MeV since its spectroscopic factor is expected to be rather small, and since the 3^+ state (2.255 MeV) is fed very strongly. The experimental data are compatible with a state around 4 MeV which is the predicted position of the second 2^+ state. We note that the calculations of the spectroscopic factors favour population of the 2^+ state rather than the known 1^+ state. However, counts in this region could arise from a different source. As shown in Fig. 2, the neutron threshold in ^{8}Li is rather low such that the t + n + ^{7}Li channel also can contribute to our spectrum. If these contributions arise from the sequence ^{9}Li(d, n)^{10}Be* followed by break-up into ^{7}Li + t, the triton energy will be recoil broadened and the angular correlations washed out.

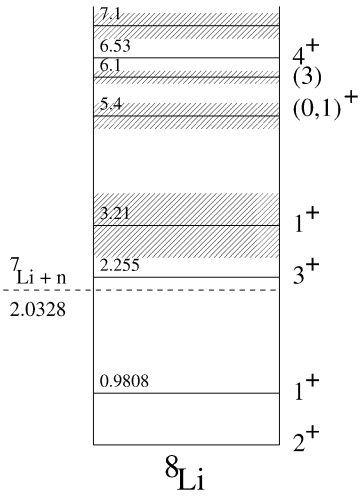

Fig. 2. The experimentally established level scheme for ^{8}Li (values from [10], energies in MeV).

The feeding patterns indicated by the theoretical spectroscopic factors are at a first glance similar to the observed spectrum below 3 MeV in Fig. 1. However, this will now be tested quantitatively with standard reaction theory.

By making selections in the excitation energy of ^{8}Li it is possible to extract differential cross sections for reactions leading to the identified states in ^{8}Li. As previously mentioned, the origin of the tritons corresponding to excitation energies larger than 3 MeV are not uniquely determined so we do not consider these data in the analysis. The differential cross section of these data are compatible with an isotropic angular distribution. The differential cross sections for the 3 states below 3 MeV are shown in Fig. 3 overlaid with optical model and compound nucleus calculations (zero degree corresponds to beam direction). Here it is worth to notice that the measured angular distribution corresponds to angles around and larger than the second diffraction maxima. Scattered tritons at forward angles, for which the dominant mechanism is expected to be the direct one, are not observed in this experiment. In contrast, at backward angles, one expects a competition between the direct and compound nucleus mechanisms. The contamination from the neighbouring states in the extracted differential cross sections are less than a few percent.

The direct contribution was calculated within the standard DWBA approach, by means of the FRESCO code [16] version frxy.3b. In prior representation, the DWBA amplitudes for our reaction reads

$$T = \langle \chi_t \phi_t | V_{[n-d]} + U_{[d-^8Li]} - U_{[d-^9Li]} | \phi_{^9Li} \chi_d \rangle, \quad (1)$$

where χ_d and χ_t are distorted waves in the entrance and exit channel, respectively, ϕ_t and $\phi_{^9Li}$ the (t|d) and (^{9}Li|^{8}Li) overlap wavefunctions, V_{n-d} is the n–d binding potential and U_{d-^8Li} is the core–core optical potential.

The optical potential for the entrance channel was taken from the analysis of the elastic data performed in [9]. The real part corresponds to a standard Woods–Saxon (WS) form, and the imaginary part to a WS derivative. The spin–orbit term of this potential, which was considered in [9], is omitted here, since it gives a negligible effect on the transfer cross section. The same optical model parameters were kept for the core–core interaction, $U_{[d-^8Li]}$, but employing $A = 8$ (^{8}Li) in the conversion from reduced to physical radii. For the neutron binding potential on either the triton or ^{9}Li nuclei, WS potentials

Table 1
Theoretical calculations of excitation energies and spectroscopic factors for low-lying states in ^{8}Li (CK from [13] and QMC from [15]). The spectroscopic factors are tabulated as SF($p_{3/2}$)/SF($p_{1/2}$)

I^π	Exp. MeV	CK MeV	QMC MeV	Spec. fact. (CK)	Spec. fact. (QMC)
2^+	0	0	0	0.885/0.012	0.966/0.114
1^+	0.9808	1.08	1.1	0.355/0.061	0.457/0.009
0^+	not obs.	4.95	2.3	0.1018/–	0.007/–
3^+	2.255	1.69	3.3	1.330/–	0.911/–
1^+	3.21	2.77	3.5	0.035/0.088	0.002/0.030
2^+	not obs.	4.24	3.8	0.047/0.296	0.014/0.107

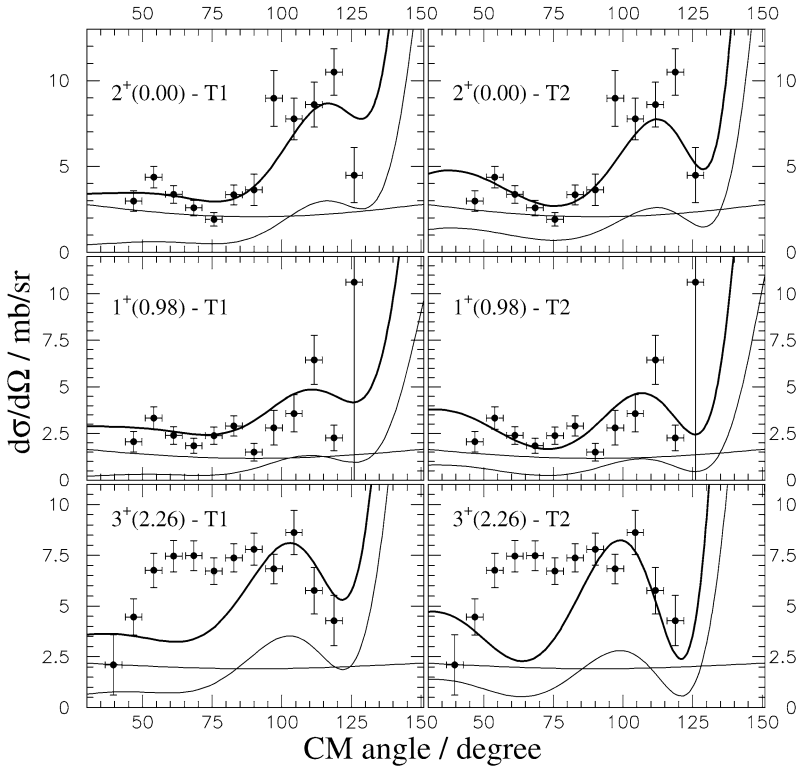

Fig. 3. Cross-section extracted for the reaction ^{9}Li + ^{2}H leading to the ground state, 1st and 2nd excited state in ^{8}Li. The calculated compound (flat line) and a finite range DWBA calculation are shown together with the fitted sum (thick line). The left and right columns correspond to the calculations with the T1 and T2 t + ^{8}Li potentials, respectively.

Table 2
Optical model parameters used in the DWBA calculations. The depth of the d + n and n + ^{8}Li potentials were adjusted to reproduce the experimental binding energy. All potentials have a derivative Woods–Saxon shape for the imaginary part except for the T2 potential, which has a volume Woods–Saxon shape

System		V_0 (MeV)	r_0 (fm)	a_0 (fm)	W_0 (MeV)	r_i (fm)	a_i (fm)	Ref.
d + ^{8,9}Li		104.6	1.2	0.65	12.4	1.2	0.65	[9]
t + ^{8}Li	T1	142	1.16	0.78	12.0	1.88	0.61	[17]
t + ^{8}Li	T2	162	1.2	0.72	16.5	1.4	0.86	[18]
n + d	B1	57.5	1.5	0.5				
n + d	B2	48.1	1.69	0.67				
n + ^{8}Li		48.32	1.27	0.67				

were used, with the depth adjusted to reproduce the experimental separation energy. In the n–d case two different geometries, denoted B1 and B2 with rms radii 2.523 and 2.737 fm, respectively, were used. Finally, two t–^{8}Li potentials were used to generate the distorted wave in the final channel. The potentials were taken from Refs. [17,18] and denoted T1 and T2, respectively. All potential parameters are listed in Table 2.

The required spectroscopic factors for the $^{9}\mathrm{Li} = {}^{8}\mathrm{Li} \otimes \mathrm{n}$ decomposition were obtained from the shell-model calculation based on the interaction of Cohen and Kurath (CK in Table 1). The triton internal wave function was assumed to be a pure s-state and hence the spectroscopic factor for the $\mathrm{t} = \mathrm{d} \otimes \mathrm{n}$ decomposition is $3/2$ [1].

The calculated transfer cross sections are compared with the data in Fig. 3 for the ground and two first excited states of ^{8}Li. These calculations use the triton binding potential B1 and the exit channel optical potential T1 or T2 (left and right column in Fig. 3, respectively) from Table 2. The pure DWBA distributions underestimate the data by a factor of up to 3. We found that, using the triton binding potential B2 instead of B1 leaves the absolute cross section and shape of the angular distribution practically unchanged (changes less than 5%). Since, to our knowledge, the elastic scattering for t + ^{8}Li has not been measured we tried different optical potentials obtained for similar systems, such as t + ^{9}Be and ^{3}He + ^{9}Be, at low energy. Although these potentials are not always consistent to each other, they systematically lead to (d, t) cross sections which are too small in comparison with the data. In particular, results with the potentials of Duggan et al. [19], Earwaker et al. [20], Kellog et al. [21] and Lamba et al. [22], gave results very similar to those obtained with the potentials T1 and T2. One has to bear in mind, however, that these potentials were derived for stable nuclei and hence their extrapolation to neutron rich nuclei might be questionable. The general underestimation of the experimen-

Table 3
Fitted scaling factors of the CK spectroscopic factors for the T1 and T2 DWBA calculations. For the 3^+ state only the 5 data points with largest scattering angles were used in the fit

I^π	E^* [MeV]	SF scaling T1	SF scaling T2
2^+	0	2.2 ± 0.3	2.6 ± 0.4
1^+	0.9808	2.3 ± 0.4	3.4 ± 0.5
3^+	2.255	1.8 ± 0.2	2.6 ± 0.2
Compound		0.9 ± 0.1	0.4 ± 0.2

tal data seen in the calculations can be improved somewhat by fitting the depths of the T2 potential (using SFRESCO), but these changes result in a worse agreement in shape, and thus these changes have been omitted.

The cross section of emitted tritons coming from the compound nucleus was estimated with the code TALYS [23]. The code EMPIRE-II [24] gives a similar relative feeding to the states in ^{8}Li and absolute cross sections within a factor of two. The angular distribution of the evaporated tritons, as predicted by the code TALYS, is plotted in Fig. 5 by the thin flat line. This contribution was found to be roughly angular-independent. It should be noted that the use of the standard compound models at this mass range can also be questioned [25]. Furthermore, it has been verified through QRPA calculations based on [26] that correlations beyond the mean-field description are small.

By adjusting the calculated differential cross sections to the data (see Fig. 3), including the compound contribution as calculated by TALYS, scaling factors for the theoretical spectroscopic factors can be extracted. For the two different set of DWBA potentials (T1 and T2) the scaling of the compound contribution was forced to be the same for all three states in ^{8}Li. The extracted scaling factors are listed in Table 3.

Fig. 3 shows that the ground state and first excited state are well described by the optical model calculations with a compound contribution within model uncertainties. The results for the second excited state seem rather different but we note that the trend in the data is very different from the compound prediction. Actually, the region 80–125 degrees can be described with an optical model calculation with a spectroscopic factor around 2 and a compound contribution of the predicted magnitude. The excess below 80° must then arise from another mechanism producing a projectile-like triton, which could originate from reactions on either ^{2}H or ^{12}C.

The scaling factors obtained in this work for the spectroscopic factors given in Table 3 are in general around two, probably indicating that our model assumptions are too simple. Inclusion of other reaction channels in a coupled channel treatment might be needed since we are in all cases close to the continuum (cf. recent results on ^{8}He + p scattering [27]). Complementary to our case are the ^{8}Li(d, p)^{9}Li reactions investigated recently at somewhat higher energy, 8 MeV/u at Argonne [28] and 5 MeV/u at Beijing [29]. The purpose of these experiments were spectroscopic and astrophysical studies of the ^{9}Li spectrum while we are considering the population of states in ^{8}Li. However, a comparison can be made for the ground state transitions, where the two inverse reactions, that both measure at small angles, agree better with calculations.

4. Summary

We were able to determine angular distributions for the three lowest states in ^{8}Li, populated in the ^{9}Li(^{2}H, t) reaction. They have been analyzed by a combination of DWBA and compound nucleus calculations. The shape of the angular distributions could be described reasonably well except for the 3^+ state where the excess at small angles may be due to projectile-like tritons. The analysis points to the importance of a precise understanding of the reaction dynamics as a necessary prerequisite for a quantitative determination of single-particle spectroscopic factors and other spectroscopic information in exotic nuclei. To conclude, in a pioneering experiment, transfer reactions at low energy with an unstable beam were performed at the REX-ISOLDE facility. The result emphasize the high potential of ISOL facilities for spectroscopic studies of exotic nuclei.

Acknowledgements

This work has been supported by the European Union Fifth Framework under contract No. HPRI-CT-1999-00018, the BMBF under contract 06 DA 115, GSI under contract DA-RIC, partly by the Spanish CICYT Agency under the project number FPA2002-04181-c04-02 as well as by the ISOLDE collaboration. Finally we would like to thank A.S. Jensen for valuable discussions.

References

[1] G.R. Satchler, Direct Nuclear Reactions, Clarendon Press, Oxford, 1983.
[2] P.E. Hodgson, Nuclear Reactions and Nuclear Structure, Clarendon Press, Oxford, 1971.
[3] C. Gund, et al., Eur. Phys. J. A 10 (2001) 85.
[4] H. Lenske, G. Schrieder, Eur. Phys. A 2 (1998) 41.
[5] S.C. Pieper, R.B. Wiringa, Annu. Rev. Nucl. Part. Sci. 51 (2001) 53.
[6] E. Kugler, Hyperfine Interact. 129 (2000) 23.
[7] D. Habs, et al., Hyperfine Interact. 129 (2000) 43.
[8] U.C. Bergmann, H.O.U. Fynbo, O. Tengblad, Nucl. Instrum. Methods Phys. Res. A 515 (2003) 657.
[9] H.B. Jeppesen, et al., Nucl. Phys. A 748 (2005) 374;
H.B. Jeppesen, PhD thesis, University of Aarhus, 2004, unpublished.
[10] D.R. Tilley, et al., Nucl. Phys. A 745 (2004) 155.
[11] S. Cohen, D. Kurath, Nucl. Phys. 73 (1965) 1.
[12] S. Cohen, D. Kurath, Nucl. Phys. A 101 (1967) 1.
[13] D. Kurath, private communication to A. Richter.
[14] S.C. Pieper, V.R. Panharipande, R.B. Wiringa, J. Carlson, Phys. Rev. C 64 (2001) 014001.
[15] R.B. Wiringa, private communication to A. Richter.
[16] I.J. Thompson, Comput. Phys. Rep. 7 (1988) 167.
[17] D.L. Powell, G.M. Crawley, B.V.N. Rao, B.A. Robson, Nucl. Phys. A 147 (1970) 65.
[18] F.D. Becchetti, G.W. Greenless, Annual Report of the J.H. Williams Laboratory of Nuclear Physics, University of Minnesota, 1969, p. 166.
[19] J.L. Duggan, et al., Nucl. Phys. A 151 (1970) 107.
[20] L.G. Earwaker, Nucl. Phys. A 90 (1967) 56.
[21] E.M. Kellog, R.W. Zurmuhle, Phys. Rev. 152 (1966) 890.
[22] C.M. Lamba, N. Sarma, N.S. Tampi, Nucl. Phys. A 122 (1968) 390.
[23] A.J. Koning, et al., in: Proceedings of International Conference on Nuclear Data for Science and Technology, Santa Fe, CA, 2004.

[24] M. Herman et al., in: Proceedings of International Conference on Nuclear Data for Science and Technology, Tsukuba, 2001.
[25] A.J. Koning, private communication.
[26] F. Hoffmann, H. Lenske, Phys. Rev. C 57 (1998) 2281.
[27] F. Skaza, et al., Phys. Lett. B 619 (2005) 82.
[28] A.H. Wuosmaa, et al., Phys. Rev. Lett. 94 (2005) 082502.
[29] B. Guo, et al., Nucl. Phys. A 761 (2005) 162.